HHS Public Access

Author manuscript

Mol Cell. Author manuscript; available in PMC 2017 February 04.

Published in final edited form as:

Mol Cell. 2016 February 4; 61(3): 419–433. doi:10.1016/j.molcel.2015.12.010.

FBXW7 facilitates non-homologous end-joining via K63-linked polyubiquitylation of XRCC4

Qiang Zhang[1], **David Karnak**[1], **Mingjia Tan**[1], **Theodore S. Lawrence**[1], **Meredith A. Morgan**[1,*], and **Yi Sun**[1,2,3,*]

[1]Division of Radiation and Cancer Biology, Department of Radiation Oncology, University of Michigan, 4424B Medical Science-I, 1301 Catherine Street, Ann Arbor, MI 48109, USA

[2]Institute of Translational Medicine, Zhejiang University School of Medicine, Hangzhou, Zhejiang, P. R. China

[3]Collaborative Innovation Center for Diagnosis and Treatment of Infectious Diseases, Zhejiang University, Hangzhou, China

SUMMARY

FBXW7 is a haploinsufficient tumor suppressor with loss-of-function mutations occurring in human cancers. FBXW7 inactivation causes genomic instability, yet the mechanism remains elusive. Here we show that FBXW7 facilitates non-homologous end-joining (NHEJ) repair and FBXW7 depletion causes radiosensitization. In response to ionizing radiation, ATM phosphorylates FBXW7 at serine 26 to recruit it to DNA double-strand break (DSB) sites, while activated DNA-PKcs phosphorylates XRCC4 at serines 325/326 which promotes binding of XRCC4 to FBXW7. SCF^{FBXW7} E3 ligase then promotes polyubiquitylation of XRCC4 at lysine 296 via K63-linkage for enhanced association with the Ku70/80 complex to facilitate NHEJ repair. Consistent with these findings, a small molecule inhibitor that abrogates XRCC4 polyubiquitylation reduces NHEJ repair. Our study demonstrates one mechanism by which FBXW7 contributes to genome integrity and implies that inactivated FBXW7 in human cancers could be a strategy for increasing efficacy of radiotherapy.

INTRODUCTION

DSBs are deleterious lesions that, if left unrepaired, can cause gross chromosomal rearrangements, genomic instability, tumorigenesis and cell death (Jackson and Bartek, 2009). While DSB repair in mammalian cells is comprised of two major and mechanistically

*Corresponding authors: Yi Sun (sunyi@umich.edu or yisun@zju.edu.cn) and Meredith A. Morgan (mmccrack@med.umich.edu).

SUPPLEMENTAL INFORMATION

Supplemental information contains seven figures and Supplemental Experimental Procedures and can be found with this article online.

AUTHOR CONTRIBUTIONS

M.A.M. and Y.S. conceived and designed this study. Q.Z. designed and performed experiments, and analyzed data. D.K and M.T. performed experiments; Q.Z, M.A.M., and Y.S. wrote the manuscript. T.S.L. contributed to the study design and manuscript editing.

distinct processes: homologous recombination (HR) and NHEJ. NHEJ represents the dominant and *a priori* DSB repair mechanism (Jeggo et al., 2011; Kakarougkas and Jeggo, 2014). In response to DSBs, NHEJ is initiated as the Ku70/80 heterodimer rapidly binds to free DNA ends and recruits the serine/threonine kinase, DNA-PKcs, followed by recruitment of Artemis, XRCC4, Ligase IV (LigIV) and XLF (Chiruvella et al., 2013; Davis and Chen, 2013; Lieber, 2010). These repair factors together with the recently identified PAXX (paralog of XRCC4 and XLF) (Ochi et al., 2015) efficiently mediate stabilization, processing, and ligation of DSBs (Lieber, 2010; Ochi et al., 2014). Defects in the core components of the NHEJ machinery, such as DNA-PKcs, LigIV, and XLF, induce radiation sensitivity (Kirchgessner et al., 1995; Shinohara et al., 2005) and genomic instability (Ferguson et al., 2000; Zha et al., 2007).

The SCF (SKP1-CUL1-F-box protein) E3 ubiquitin ligase consists of the adaptor protein SKP1, the scaffold protein Cullin-1, a substrate recognizing subunit or F-box protein, and the RING component RBX1 or RBX2. While RBX1/RBX2 is required for ligase activity by transferring the ubiquitin from an E2 to the substrate, the F-box protein determines the substrate specificity (Deshaies and Joazeiro, 2009). The human genome contains 69 F-box proteins (Jin et al., 2004), which recognize hundreds of protein substrates. By promoting the ubiquitylation of various protein substrates for targeted proteasomal degradation, SCF E3 controls many important biological processes, including cell cycle progression, DNA replication, and tumorigenesis (Jia and Sun, 2011; Nakayama and Nakayama, 2006; Zhao and Sun, 2013). However, knowledge regarding the role of SCF E3 in DSB repair is limited, although several single component RING-type E3 ubiquitin ligases, such as RNF8 and RNF168, have been shown to promote K63-linked ubiquitylation of histones and subsequent recruitment of DSB repair factors, such as BRCA1 and 53BP1 to DSB sites (Bartocci and Denchi, 2013; Ulrich and Walden, 2010).

FBXW7 is a well-characterized substrate recognition subunit of the SCF E3 ubiquitin ligase which has previously been found to function exclusively by K48-ubiquitylation and subsequent degradation of target proteins (Nakayama and Nakayama, 2006; Welcker and Clurman, 2008). Several oncogenic proteins, such as Cyclin E, c-JUN and c-MYC are substrates for SCF^{FBXW7}-mediated degradation, thus conferring the tumor suppressor functions of FBXW7 (Welcker and Clurman, 2008). Likewise, loss-of-function mutation of FBXW7 is frequently found in human cancers (Akhoondi et al., 2007; Calhoun et al., 2003; Davis et al., 2014; Jones et al., 2008; Wang et al., 2014; Welcker and Clurman, 2008). Genetic inactivation of FBXW7 causes chromosomal instability characterized by aneuploidy and micronuclei formation (Rajagopalan et al., 2004), and is associated with increased radiation-induced tumorigenesis (Mao et al., 2004). However, whether and how FBXW7 functions in the DSB repair process for the maintenance of genomic integrity is unknown.

In this study we found that FBXW7 enhances NHEJ repair. Upon DNA damage by ionizing radiation, FBXW7 is phosphorylated at serine 26 by ATM and then recruited to DSB sites where it ubiquitylates XRCC4 via K63-linkage at lysine 296 to facilitate the association of XRCC4 with the Ku70/80 heterodimer, thus promoting NHEJ repair. FBXW7 inactivation via genetic or pharmacological approaches inhibits NHEJ repair and sensitizes cancer cells to radiation.

RESULTS

FBXW7α is recruited to DSBs in an ATM-dependent manner

To determine the role of FBXW7 in the maintenance of genomic integrity, we investigated its involvement in the DNA damage response and repair process, since DNA repair machinery is critical to maintain genome stability (Ferguson et al., 2000; Zha et al., 2007). Indeed, upon radiation, FBXW7 formed punctuate nuclear foci, which partially co-localized with 53BP1 foci (Figure 1A). UVA laser microirradiation revealed rapid kinetics of FBXW7 recruitment to DNA damage sites, occurring as early as 1 minute and peaking at 10–20 minutes (Figure 1B). Thus, FBXW7 directly participates in the initial phase of cellular DNA damage responses by localizing to DNA damage sites. FBXW7 has three isoforms (α, β, and γ) varying only in their N-terminal region and consequently, their subcellular localization (nucleus, cytoplasm, and nucleolus, respectively) which likely confers compartment-dependent substrate specificity (Grim et al., 2008; Welcker and Clurman, 2008). Importantly, only the nuclear isoform FBXW7α contains two evolutionarily conserved serine/glutamine (SQ) motifs (S26 and S72), which are potential phosphorylation sites of ATM/ATR/DNA-PKcs-like kinases (Figures S1A and S1B). Furthermore, only FBXW7α localizes to DNA damage sites, while FBXW7β and FBXW7γ do not (Figure S1C). We then determined whether these SQ motifs unique to FBXW7α are phosphorylated in response to radiation by immunoprecipitation-coupled immunoblotting with p-S/TQ antibody. Remarkably, FBXW7 was rapidly phosphorylated within 1 minute and reached maximal levels within 15–30 minutes post-radiation (Figure 1C), kinetics which are consistent with FBXW7 recruitment to DNA damage sites. We then identified the kinase(s) for FBXW7 phosphorylation using selective inhibitors against DNA-PKcs, ATM and ATR (Figure S1D). While inhibitors of DNA-PKcs and ATR had minimal effect on FBXW7 phosphorylation at the SQ motif, the ATM inhibitor KU55933 completely eliminated radiation-induced FBXW7 phosphorylation at S/TQ sites (Figure 1D). Inhibition of CK1 or CDK1, two kinases predicted by computer algorithms to phosphorylate FBXW7 at S26, did not affect FBXW7 phosphorylation (Figure S1E), suggesting that FBXW7 is a direct substrate of ATM. Furthermore, FBXW7 localization to DNA damage sites was inhibited by KU55933 (Figure S1F), indicating a requirement of ATM-induced phosphorylation at the SQ motif for FBXW7 recruitment. We further confirmed ATM requirement using genetic approaches and found that, in contrast to ATM wild type fibroblasts, FBXW7 in ATM null fibroblasts (derived from an ataxia-telangiectasia patient) failed to localize to DNA damage sites, whereas localization of 53BP1 positive control was unaffected (Figure 1E). Finally, we defined which SQ site is phosphorylated by ATM using two FBXW7 single mutants, FBXW7-S26A and FBXW7-S72A, and found that radiation-induced FBXW7 phosphorylation was completely abrogated in the FBXW7-S26A mutant, but not in the FBXW7-S72A mutant (Figure 1F). Consistent with this result, the phosphorylation-sensitive FBXW7-S72A mutant was recruited to microirradiation-induced DNA damage sites with an intensity similar to that of the wild type, whereas recruitment of the phosphorylation-resistant FBXW7-S26A mutant was remarkably reduced, if not completed eliminated (Figure 1G). Thus, upon DNA damage, activated ATM phosphorylates FBXW7 on serine 26 to facilitate its recruitment to DNA damage sites.

FBXW7 regulates non-homologous end-joining and radiosensitivity

We next determined the biological significance of FBXW7 recruitment to DNA damage sites, using γH2AX as a readout (Lobrich et al., 2010) in paired FBXW7$^{+/+}$ and FBXW7$^{-/-}$ tumor cells. The γH2AX levels were significantly elevated in FBXW7$^{-/-}$ cells compared to FBXW7$^{+/+}$ cells following radiation (Figure 2A), a result confirmed in multiple model systems including isogenic (Figure S2A and S2B) and siRNA-treated cells (Figures 2B, S2C, and S2D). To determine whether the persistent DNA damage seen in FBXW7 deficient cells was due to defective DSB repair, we assessed the effects of FBXW7 depletion on both HR and NHEJ repair. Using both a reporter of homology-directed repair (Pierce et al., 1999) as well as RAD51 focus formation, FBXW7 depletion had no effect on HR (Figures 2C, 2D, and S2E, respectively). We then focused on NHEJ repair. Pancreatic cancer cells treated with non-specific or FBXW7 siRNA were transfected with linearized pEYFP DNA, and NHEJ assessed by quantitative real-time PCR of the re-ligated EYFP sequence (Deans et al., 2006). FBXW7 depletion significantly inhibited NHEJ in both MiaPaCa-2 (Figure 2E) and Panc-1 cells (Figure S2F). Furthermore, in pancreatic cancer cells constructed to stably express an NHEJ reporter that measures repair of an I-SceI-induced DSB by GFP expression (Mao et al., 2009), depletion of FBXW7 by siRNAs significantly inhibited NHEJ (Figures 2F and S2G). Finally, we incubated linearized plasmid DNA (EcoRI, 5′ overhangs) with cell-free extracts (Budman and Chu, 2006) from two FBXW7 isogenic pairs of cells and found reduced end-joining products in FBXW7$^{-/-}$ HCT116 and DLD1 cells (Figure 2G). Importantly, we found that stable expression of wild type FBXW7α completely rescued the NHEJ defect observed in FBXW7$^{-/-}$ cells, while FBXW7α S26A mutant had significantly reduced NHEJ activity relative to wild type (Figures 2H and S2H). To determine the biological significance of the role of FBXW7 in NHEJ repair, we assessed the effects of FBXW7 deficiency on radiation survival. In multiple cell lines (MiaPaCa-2, HCT116, Panc-1, DLD1), FBXW7 deficiency (either via siRNA-mediated depletion or genomic deletion) caused significant radiosensitization (Figures 2I, 2J, S2I, and S2J), suggesting that FBXW7 could be a target for radiosensitization of cancer cells. Taken together, our results demonstrate ATM-dependent FBXW7 recruitment to DSB sites to promote NHEJ (but not HR) repair and survival following radiation-induced DNA damage.

We also extended this observation to normal cells by assessing the effects of FBXW7 deficiency on γH2AX focus formation and NHEJ activity. Mouse Fbxw7 was depleted in mouse embryonic fibroblasts (MEF) by Ad-Cre infection of MEF cells derived from Fbxw7$^{fl/fl}$ embryos (Figures 2K) and human FBXW7 was depleted by siRNA silencing in human fibroblast cell lines (HFF and MRC5) (Figure S2K). Cells were then synchronized in the G1 phase of the cell cycle to more clearly distinguish NHEJ defects. Fbxw7$^{-/-}$ MEF cells exhibited significantly higher levels of γH2AX foci 2 hours post-radiation than Fbxw7$^{+/+}$ cells (Figures 2K and 2L). Similarly, depletion of FBXW7 from human fibroblast cells caused significantly higher levels of γH2AX at 2 hours post-irradiation (Figures S2L and S2M), which is likely attributable to impaired NHEJ repair, as NHEJ activity is significantly reduced in FBXW7 depleted cells (Figures 2M and 2N). These results demonstrate that the function of FBXW7 in NHEJ repair is maintained in normal cells.

SCF^{FBXW7} promotes XRCC4 polyubiquitylation via K63-linkage

To determine how FBXW7 promotes NHEJ repair, we first investigated Cyclin E, an FBXW7 substrate that was previously linked to genomic instability in FBXW7 deficient cells (Akhoondi et al., 2007). As expected, Cyclin E protein levels were higher in $FBXW7^{-/-}$ cells (Figure S3A). However, Cyclin E depletion did not rescue the NHEJ defect in $FBXW7^{-/-}$ cells, suggesting a Cyclin E-independent mechanism (Figure S3B). We then focused our investigation on core NHEJ proteins, and found using immunoprecipitation assays, that in response to radiation, FBXW7 interacted rather specifically with the LigIV/XRCC4/XLF complex since it failed to interact with other DSB repair associated proteins such as MDC1 and 53BP1 (Figures 3A and S3C). Furthermore, the recruitment of other DSB repair proteins including 53BP1 and MRE11 remained intact in $FBXW7^{-/-}$ cells (Figure S3D). To define the direct FBXW7 binding partner in the LigIV/XRCC4/XLF complex, we searched for FBXW7 conserved binding motifs on all three proteins, and identified an evolutionarily conserved putative binding motif (RNSSPED) on XRCC4 (Figure S3E). Indeed, in response to DNA damage, endogenous FBXW7 bound to endogenous XRCC4 as demonstrated by reciprocal co-immunoprecipitation with XRCC4 antibody (Figure 3B). Furthermore, FBXW7-XRCC4 binding was dependent on serine residues within the putative binding motif, since their mutation (S325A and S326A) dramatically inhibited their binding (Figure 3C).

As FBXW7 is a substrate recognition component of the SCF E3 ubiquitin ligase, we next determined whether FBXW7 promotes XRCC4 ubiquitylation. Indeed, we found that FBXW7 mediated XRCC4 ubiquitylation in response to radiation (Figures 3D and S3F). Furthermore, we assessed the dependency on the Cullin-1 subunit of the SCF^{FBXW7} and found, as anticipated, reduced XRCC4 ubiquitylation following siRNA-mediated depletion of Cullin-1 (Figure S3G). Consistent with the effects of FBXW7 depletion, Cullin-1 depletion also caused NHEJ inhibition (Figure S3H). Furthermore, Cullin-1 was found in the XRCC4-FBXW7 complex (Figure 3B). Together, these findings suggest that XRCC4 ubiquitylation and NHEJ activity are regulated by the SCF^{FBXW7} E3 ubiquitin ligase.

In all known cases, FBXW7 recognizes and binds its substrates, followed by targeted ubiquitylation and subsequent degradation (Nakayama and Nakayama, 2006; Welcker and Clurman, 2008). We therefore examined the protein half-life of XRCC4 in both $FBXW7^{+/+}$ and $FBXW7^{-/-}$ cells, and found that XRCC4, like other core NHEJ proteins, was relatively stable with a half-life greater than 18 hours (Figure S3I). Furthermore, depletion of FBXW7 had little, if any, effect on its half-life, regardless of radiation exposure (Figure S3J), indicating that the binding of FBXW7 to XRCC4 did not promote its degradation. Recent studies have shown that non-proteolytic ubiquitylation at regions flanking DNA damage sites plays a crucial role in the DNA damage response, which is mediated by K63-linked ubiquitylation, a major genotoxic stress-induced modification (Chen and Sun, 2009; Ulrich and Walden, 2010). We therefore determined the linkage site of the polyubiquitylation chain on XRCC4 using two ubiquitin mutants, K48R and K63R. We found that FBXW7 promoted K63-linked, rather than K48-linked ubiquitylation of XRCC4, since K63, but not K48 mutation completely abrogated XRCC4 polyubiquitylation (Figure 3E). To further verify K63-linked ubiquitylation of XRCC4 by FBXW7, ubiquitin mutants were used which

contain only a single wild type lysine (K48 or K63) with all other lysines mutated to arginine. Similar to wild type ubiquitin, K63 only mutant showed substantial XRCC4 polyubiquitylation, whereas no XRCC4 polyubiquitylation was observed, when a K48 only mutant was used (Figure 3F). These results are further supported by the finding that siRNA-mediated depletion of UBC13, an E2 which predominantly mediates K63-linked polyubiquitylation (Hofmann and Pickart, 1999; VanDemark et al., 2001), but not UBC5, an E2 for K48-linked polyubiquitylation, completely abrogated FBXW7-mediated XRCC4 polyubiquitylation (Figure 3G). Furthermore, UBC13 was found in FBXW7-XRCC4 complex (Figure 3A) and siRNA silencing UBC13, but not UBC5, inhibited NHEJ repair (Figure 3H). Taken together, these results demonstrate that FBXW7 interacts with the LigIV/XRCC4/XLF NHEJ protein complex via direct binding with XRCC4 to promote its polyubiquitylation via the K63-linkage, which may in turn promote NHEJ repair.

SCF^{FBXW7} ubiquitylates XRCC4 at Lys296 in an ATM- and DNA-PKcs-dependent manner

Having established XRCC4-S325/326-dependent binding between FBXW7 and XRCC4 (Figure 3C), which is consistent with the notion that phosphorylation of substrate binding motifs is a prerequisite for substrate recognition by an F-box protein (Zhou et al., 2013), we next determined if XRCC4 polyubiquitylation is also dependent on S325/326 phosphorylation. Indeed, polyubiquitylation promoted by UBC13 was observed only in response to wild type XRCC4, with no or substantially reduced polyubiquitylation in the S325/326A mutant (Figures 4A and S4A). Since DNA-PKcs is a known kinase for S325/326 phosphorylation on XRCC4 (Yu et al., 2003), we inactivated DNA-PKcs by pharmacological (NU7441) (Figure 4B) or genetic (siRNA) (Figure 4C) approaches and found a dramatic reduction of XRCC4 polyubiquitylation, indicating that radiation-induced, FBXW7-mediated XRCC4 polyubiquitylation is DNA-PKcs dependent. As expected, ATM inactivation by KU555933 treatment or by siRNA also markedly inhibited XRCC4 polyubiquitylation (Figures 4B and 4C) via abrogation of FBXW7 phosphorylation and recruitment to DNA damage sites (Figure 1D–G).

We further defined the potential lysine residue on which XRCC4 ubiquitylation occurs. Based upon the available crystal structure of XRCC4 and known domains which bind to other NHEJ components (Junop et al., 2000), we made four XRCC4 K→R mutants on evolutionarily conserved lysine residues at the C-terminus with an open β-sheet structure, free of binding to other NHEJ proteins (Figure S4B). Among all four mutants, only K296R mutation completely abrogated FBXW7-mediated polyubiquitylation (Figure 4D), indicating that the K296 residue is the ubiquitylation site on XRCC4. We also found a reduced XRCC4 polyubiquitylation in K271R mutant, which is likely due to introduction of a mutation in the nuclear localization signal (NLS) motif (Figure S4C, underlined sequence), which substantially reduced its nuclear localization (Figure S4D), thus limiting its polyubiquitylation by nuclear FBXW7α. Our finding is consistent with a recent report (Fukuchi et al., 2015). Taken together, these data demonstrate that in response to DNA damage, FBXW7 binds to and ubiquitylates XRCC4 at K296 via K63-linkage in an ATM and DNA-PKcs-dependent manner to promote NHEJ.

FBXW7-XRCC4 polyubiquitylation facilitates NHEJ complex formation, XRCC4 localization to DSBs, and NHEJ repair

To determine how FBXW7 and FBXW7-mediated K63-linked XRCC4 polyubiquitylation promotes NHEJ, we assessed the effects of FBXW7 on interactions among core NHEJ components. While we found that the interaction among XRCC4, LigIV, and XLF was comparable between FBXW7$^{+/+}$ and FBXW7$^{-/-}$ cells, the association of XRCC4 with the Ku70/80 heterodimer was remarkably reduced in FBXW7$^{-/-}$ cells (Figures 5A, S5A and S5B). This finding was confirmed by reciprocal co-immunoprecipitation with Ku80 antibody which showed a reduced interaction of Ku80 with XRCC4, LigIV, and XLF in FBXW7$^{-/-}$ cells (Figure 5B), suggesting that FBXW7-mediated XRCC4 polyubiquitylation facilitates the interaction between XRCC4/LigIV/XLF and Ku70/80 complexes. In addition, we found that XRCC4 polyubiquitylation is required for XRCC4 to form a complex with Ku70/80, since the ubiquitin site mutant, XRCC4-K296R failed to bind to Ku80 and displayed substantially reduced binding to Ku70, while binding with LigIV and XLF was unaltered (Figure 5C). Finally, having established that XRCC4 ubiquitylation promotes XRCC4 and Ku70/80 interaction, we assessed the ability of Ku70/80 to bind to synthetic tetra-ubiquitin peptides with different lysine linkages and found that Ku70/80 directly bound K63-linked tetra-ubiquitin with very minimal binding to K48-linked tetra-ubiquitin (Figure 5D), suggesting that the interaction between ubiquitylated XRCC4 and Ku70/80 is through a K63-linkage ubiquitin binding domain in Ku70/80.

Ubiquitylation at K296 promotes XRCC4 chromatin association, NHEJ repair, and radiation survival

We next determined the effect of FBXW7 on recruitment and/or retention of XRCC4 to DSBs by measuring GFP-XRCC4 localization to microirradiation-induced DNA damage sites. Although GFP-XRCC4 was rapidly recruited to DNA damage sites (within 60 seconds) in both FBXW7$^{+/+}$ and FBXW7$^{-/-}$ cells, the amount of XRCC4 recruited, as reflected by fluorescent intensity along the laser track, was significantly reduced in the absence of FBXW7 (Figure 6A). Furthermore, the K296R mutant also displayed significantly reduced recruitment to DNA damage sites (Figure 6B). Consistent with these data, chromatin fractionation studies revealed decreased chromatin binding of the XRCC4-K296R mutant in response to radiation-induced DNA damage (Figure 6C), as well as reduced XRCC4 chromatin binding in FBXW7$^{-/-}$ cells following radiation (Figure S6A). These data provide evidence from two independent endpoints, that FBXW7 is required for efficient recruitment of XRCC4 to DNA damage sites.

To determine the functional consequences of mutations on the sites of XRCC4 phosphorylation and ubiquitylation, we performed a rescue experiment by measuring NHEJ activity in XRCC4$^{-/-}$ cells expressing wild type or XRCC4 mutants, S325/326A or K296R, along with a vector control (Figure S6B). Wild type XRCC4 completely rescued NHEJ, as expected, whereas XRCC4 mutants, S325/326A or K296R conferred a partial rescue, as evidenced by significantly reduced NHEJ activity (Figure 6D). The biological effects of XRCC4 mutation (K296 or S325/326) were assessed in radiation survival assays which demonstrated that XRCC4 S325/326A and K296R are compromised in their ability to rescue radiosensitization relative to wild type XRCC4 in XRCC4$^{-/-}$ cells (Figure 6E). It is worth

noting that depletion of XRCC4, a core component of the NHEJ complex, renders cells more sensitive to radiation than depletion of FBXW7, which acts as a facilitator of NHEJ repair, as evidenced by greater radiosensitization in XRCC4 null cells than in FBXW7 null cells (RER 2.2 vs 1.5, respectively, Figures 6E and 2I) as well as more severe defects in DNA damage repair, reflected by γH2AX positivity (Figure S6C) and NHEJ activity (Figures 2M and 2N). Taken together, these results clearly demonstrate that FBXW7-mediated XRCC4 polyubiquitylation at K296 facilitates XRCC4 interactions with Ku70/80 and its recruitment to chromosomal DSBs for effective NHEJ repair and survival following radiation-induced DNA damage.

Pharmacological inhibition of SCF^{FBXW7} leads to defective NHEJ

To determine whether the functions of SCF^{FBXW7} in NHEJ repair could be targeted pharmacologically, we utilized MLN4924, a small molecule inhibitor of the NEDD8-activating enzyme, currently in Phase 1–2 clinical trials, which inhibits Cullin-1 neddylation and thus, SCF activity (Nawrocki et al., 2012; Soucy et al., 2009; Zhao et al., 2014). Indeed, MLN4924 effectively abrogated FBXW7-mediated K63-linked polyubiquitylation of XRCC4 (Figures 7A and S7A), and inhibited NHEJ repair under the concentrations in which cullin-neddylation was near completely abrogated, but with little to no effect on the levels of core NHEJ proteins (Figures 7B, S7B, and S7C). MLN4924 also inhibited NHEJ in a concentration-dependent manner in other independent NHEJ repair assays and with an activity comparable to the DNA-PKcs inhibitor, Nu7741 (Zhao et al., 2006) (Figures 7C, 7D, S7D, and S7E). The effect of MLN4924 on NHEJ was greater in cells expressing FBXW7 than in cells depleted of FBXW7 (Figure 7E), supporting the involvement of the FBXW7/XRCC4 axis in NHEJ inhibition by MLN4924. Finally, MLN4924 reduced the binding between XRCC4 and Ku70/80 (Figure S7F). Collectively, these findings are consistent with our previous studies demonstrating that MLN4924 induces significant radiosensitization of cancer cells both *in vitro* and *in vivo* in association with persistent DSBs (Wei et al., 2012). Furthermore, these findings demonstrate that MLN4924 can be used to inhibit K63-linked ubiquitylation and NHEJ repair.

DISCUSSION

FBXW7 is a prototypical tumor suppressor which is inactivated in many human cancers, and its inactivation is associated with reduced patient survival (Davis et al., 2014; Wang et al., 2014; Welcker and Clurman, 2008). The tumor suppressor function of FBXW7 is thought to be attributable to its degradation of a number of oncogenic proteins, including c-JUN, c-MYC, Cyclin E, Notch, and MCL-1 (Davis et al., 2014; Wang et al., 2014; Welcker and Clurman, 2008). On the other hand, it has been known for more than a decade that FBXW7 is required for the maintenance of genomic stability (Rajagopalan et al., 2004), but how FBXW7 acts in that regard is unknown, although accumulation of Cyclin E and Aurora-A was implicated (Perez-Losada et al., 2005; Rajagopalan et al., 2004). Here we report a Cyclin E-independent function of FBXW7. Instead, in our system FBXW7 preserves genomic integrity by localizing to DNA damage sites, where it promotes polyubiquitylation of phosphor-XRCC4 via K63-linkage to enhance Ku70/80 binding, thus facilitating NHEJ repair. We provide the following evidence to support this conclusion. 1) Upon radiation-

induced DNA damage, FBXW7 is phosphorylated at S26 by ATM and rapidly recruited to DNA damage sites; 2) XRCC4 is phosphorylated by DNA-PKcs at S325/S326 which facilitates FBXW7 binding; 3) SCF^{FBXW7} then promotes XRCC4 polyubiquitylation at K296 via a K63 linkage; 4) polyubiquitylated XRCC4 has enhanced interaction with the Ku70/80 complex and DNA damage sites to promote NHEJ repair, whereas the ubiquitin-resistant XRCC4-K296R mutant, along with the recruitment-deficient FBXW7-S26A mutant and phosphorylation-resistant XRCC4-S325A/S326A mutant, have significantly reduced NHEJ repair capacity; 5) inactivation of FBXW7 via genetic or pharmacological approaches abrogates NHEJ repair and renders cells more sensitive to DNA damaging agents, such as ionizing radiation. Herein, we report the direct involvement of FBXW7 in DSB repair, and provide evidence that FBXW7 can cause substrate polyubiquitylation via K63-linkage for functional modulation. Our study supports the working model shown in Figure 7F, and further suggests that FBXW7 inactivation by either loss-of-function mutation or pharmacological inhibition could increase the efficacy of radiotherapy of human cancers. This is supported by the findings that FBXW7 mutation is associated with increased radiosensitivity (Figure S7G) and that pharmacological inhibition of SCF^{FBXW7} induces radiosensitization (Wei et al., 2012). Involvement of SCF E3 ubiquitin ligases in DSB repair has been implicated in a few recent studies. For example, Cullin-1 depletion leads to DSBs and γH2AX focus formation (Cukras et al., 2014). Removal of Ku from DSBs following NHEJ is neddylation-dependent and blocked by MLN4924 treatment (Brown et al., 2015). More specifically, SCF^{SKP2} was found to mediate K63-linked ubiquitylation of NBS1 to promote its association with ATM to enhance HR repair (Wu et al., 2012). $SCF^{\beta TRCP}$ was reported to promote degradation of XLF to disrupt XRCC4/XLF/LigIV complex and abrogate NHEJ (Liu et al., 2015). Our finding provides yet another mechanism by which SCF^{FBXW7} E3 ubiquitin ligase regulates genomic stability and DNA repair by promoting XRCC4 polyubiquitylation via K63-linkage for effective NHEJ repair.

NHEJ is a major repair pathway for DSBs and its defect causes radiation sensitivity and genomic instability (Rooney et al., 2003; Woodbine et al., 2014), NHEJ repair is tightly regulated by a series of interactions between two core complexes of the machinery, including the Ku70/80 heterodimer/DNA-PKcs complex and the XRCC4/Lig IV/XLF complex (Mari et al., 2006; Ochi et al., 2014). However, the mechanisms by which these proteins assemble into functional protein-DNA complexes remain elusive (Ochi et al., 2014; Radhakrishnan et al., 2014; Williams et al., 2014). It has been demonstrated that the direct association of Ku70 and XRCC4 is weak in biochemical assays (Mari et al., 2006). Our finding therefore, provides a mechanism by which SCF^{FBXW7}-mediated XRCC4 polyubiquitylation could enhance the binding of XRCC4 to the Ku70/80 heterodimer to facilitate NHEJ repair in response to DSBs.

XRCC4 is a nuclear phosphoprotein, which is phosphorylated by DNA-PKcs in response to radiation (Critchlow et al., 1997). A prior study examined the function of these phosphorylation sites in the radiation survival of XR-1 cells (a DSB repair mutant cell line derived from CHO cells which lacks XRCC4) and found that expression of XRCC4 containing a combination of six serine to alanine mutations (including S325/326A) was able to rescue radiation survival in this model (Yu et al., 2003). Ubiquitylation of XRCC4 has also been previously reported, and an increase in the abundance of ubiquitylated XRCC4

was observed when cells were exposed to genotoxic stress (Foster et al., 2006). Until now, however, the function of XRCC4 ubiquitylation and the E3 ligase responsible for XRCC4 ubiquitylation were unknown. Our study clearly demonstrates that upon DNA damage, activated DNA-PKcs phosphorylates XRCC4 at S325/326 to facilitate its binding to FBXW7 for targeted polyubiquitylation by SCF^{FBXW7} E3 ligase.

We have previously shown that the NEDD8-activating enzyme inhibitor MLN4924 sensitizes pancreatic cancer cells to radiation via inhibition of SCF ligase activity resulting in accumulation of SCF substrates, CDT1 and WEE1 (Wei et al., 2012). Similarly, others have shown that accumulation of proteins involved in DNA replication, DNA damage response and repair is critical to the lethality of MLN4924 (Blank et al., 2013; Garcia et al., 2014). In contrast to these studies which largely implicate inhibition of K48-linked ubiquitylation and protein degradation to the activity of MLN4924, here, we show that MLN4924 can also modulate K63-linked ubiquitylation. This finding provides another mechanism of MLN4924 that causes inhibition of NHEJ repair and radiosensitization. Therapeutically, MLN4924 has been utilized to inhibit protein degradation of Cullin-RING ligase substrates due to K48-linked ubiquitylation (Soucy et al., 2009; Zhao et al., 2014). Given the emerging non-proteolytic functions of SCF E3 ubiquitin ligases in DSB repair, described in the current and one prior report (Wu et al., 2012), MLN4924 represents an important therapeutic strategy for inhibiting both NHEJ (via SCF^{FBXW7}) and potentially, HR (via SCF^{SKP2}) and sensitizing tumor cells to DNA damage. Finally, the concentration-dependent inhibition of NHEJ by MLN4924 in FBXW7 null cells (Figure 7E) suggests the involvement of other CRL substrates.

FBXW7 is a tumor suppressor whose loss-of-function mutations, which are frequently found in human cancers, would cause accumulation of oncogenic substrates such as Cyclin E, c-JUN, c-MYC, MCL-1, and Notch to promote tumorigenesis (Davis et al., 2014). Notably, unlike depletion of core NHEJ proteins which causes severe radiation sensitivity, depletion of FBXW7 leads to moderate, yet significant radiation sensitivity. This is likely due to the counteracting effect of accumulation of other FBXW7 substrates such as c-MYC, MCL-1, and Notch, which confer radioresistance (Theys et al., 2013; Wang et al., 2010; Wang et al., 2013; Wei et al., 2015). Nevertheless, we show that abrogation of K63 linked polyubiquitylation of XRCC4 upon FBXW7 inactivation is an important contributor to cellular radiation sensitivity, which overcomes the radioresistant effect of other FBXW7 substrates, resulting in a net outcome of radiosensitization.

In summary, our study not only identifies functions of FBXW7 in regulating NHEJ, but also provides a rationale for enhancing the efficacy of radiation therapy by FBXW7 inactivation. Specifically, human cancer cells with loss-of-function mutations in FBXW7 or pharmacologically inactivated FBXW7 might be more sensitive to radiation and possibly other DNA damaging chemotherapies due to defective NHEJ repair.

EXPERIMENTAL PROCEDURES

Immunofluorescence

For immunofluorescence experiments, cells were grown and treated on cover slips in 12-well dishes. Following treatment, cells were fixed and stained as previously described (Karnak et al., 2014) with antibodies recognizing γH2AX, 53BP1 (Millipore), RAD51 (GeneTex), or MRE11 (Cell Signaling) and DAPI (4′,6-diamidino-2-phenylindole). Samples were imaged with an Olympus IX71 FluoView confocal microscope (Olympus America) with a 60x oil objective. Fields were chosen at random based on DAPI staining. For quantitation of RAD51 foci, at least 100 cells from each treatment condition were visually scored. Cells with 5 or more RAD51 foci were scored as positive.

Microirradiation

Cells were seeded onto glass-bottom dishes (MatTek) and transfected with pEGFP-FBXW7α (WT and mutants) or pEGFP-XRCC4 (WT and mutants). GFP-positive cells were then irradiated with a 365-nm UVA laser focused through a 60x/1.2-W objective using a Zeiss Axiovert equipped with LSM 520 Meta. UVA (4.36 J/m2) was introduced to an area of approximately 12 μm × 0.1 μm. Images were captured at 1 min intervals.

Ubiquitylation assays

In vivo and *in vitro* ubiquitylation assays were performed as previously described (Wu et al., 2012; Zhao et al., 2011). For *in vivo* ubiquitylation assays MiaPaCa-2 cells were transfected with the indicated plasmids for 48 hours and then harvested in cell lysis buffer. The cell extracts were then incubated with HA beads for 3 hours, washed, and subjected to immunoblot analysis. For *in vitro* ubiquitylation assays HA-XRCC4 proteins and Flag-FBXW7α-SCF complex isolated from MiaPaCa-2 cell lysates (IR-treated) were incubated with 0.5 mg E1 (Boston Biochem), 1.5 mg ubiquitin (Boston Biochem), 1 mg UBC13/UEV1A (Boston Biochem), and 2.5 mM ATP in a final 30 ml reaction buffer (1.5 mM MgCl2, 5 mM KCl, 1 mM DTT, 20 mM HEPES [pH 7.4]) at 30 °C for 2 hours. XRCC4 ubiquitylation was detected by immunoblotting.

NHEJ assay in cell-free extracts

The NHEJ assay was performed as described with modifications (Pfeiffer et al., 2014; Sharma and Raghavan, 2010). In brief, cell-free extracts (0.5 μg) were incubated with pBlueScript plasmid linearized by different restriction enzymes (Supercoiled pBluescript SK + (3.0 Kb) was digested with EcoRI to generate DSBs with 5′ overhangs, PstI to generate 3′ overhangs, or EcoRV to generate blunt ends.) in NHEJ buffer (25 mM Tris-HCl, [pH 7.5], 75 mM NaCl, 10 mM $MgCl_2$, 42.5 mM KCl, 0.025% Triton X-100, 100 μg/ml BSA, 10% PEG, and 5% glycerol) in a reaction volume of 10 μl at 25°C for 30 minutes. Reactions were terminated by addition of EDTA (10 mM) and products were purified by phenol-chloroform extraction followed by precipitation. Reaction products were purified and resolved on a 2% agarose gel and visualized by ethidium bromide staining.

NHEJ linearized plasmid assay

For the linearized plasmid-based end-joining assay, pEYFP-N1 (Clontech Laboratories Inc., Mountain View, CA) was linearized by digesting between the promoter and coding sequence of YFP with NheI. The linear products were gel purified and transfected into serum starved (overnight) cells. After 12 hours, cells were harvested and lysed to isolate transfected plasmids. The efficiency of end-joining repair was assessed by qPCR of the ligated YFP region, normalized to an uncut flanking DNA sequence, relative to control siRNA or DMSO-treated cells.

NHEJ I-SceI reporter assay

The I-SceI-based NHEJ assay was performed as described earlier with modifications (Mao et al., 2009). Cells stably expressing the NHEJ reporter (2×10^4) were seeded in 12-well plates. Cells transfected with various siRNAs or treated with different drugs were infected with I-SceI-expressing adenovirus. Media was changed (with drugs) after 18 hours to avoid adenovirus toxicity. Cells were harvested for FACS analysis after 24 hours. The percentage of GFP-positive cells (indicative of NHEJ repair) was quantitated by flow cytometry.

Statistics

Statistically significant differences for the clonogenic survival and immunofluorescence assays were determined by one-way ANOVA with the Tukey post-comparison test in GraphPad PRISM version 5 (GraphPad software). For γH2AX, NHEJ and HR repair assays, a Student's, two-tailed *t* test was performed in GraphPad PRISM.

Supplementary Material

Refer to Web version on PubMed Central for supplementary material.

Acknowledgments

We thank Drs. Xiaochun Yu, JoAnn Sekiguchi, and Christine Canman for generously providing instruments, reagents and helpful discussions. We also thank Dr. Iannis Aifantis for providing $Fbxw7^{fl/fl}$ mice, and Drs. Mukesh Nyati, Dipankar Ray, Bert Vogelstein, and Ping Wang for cell lines and reagents and Joshua Parsels and Jason Schreiber for technical support. This work is supported by NIH Grant R01CA163895 (M.A.M.) and R01 CA118762, CA156744, and CA171277 (Y.S.).

References

Akhoondi S, Sun D, von der Lehr N, Apostolidou S, Klotz K, Maljukova A, Cepeda D, Fiegl H, Dafou D, Marth C, et al. FBXW7/hCDC4 is a general tumor suppressor in human cancer. Cancer Res. 2007; 67:9006–9012. [PubMed: 17909001]

Bartocci C, Denchi EL. Put a RING on it: regulation and inhibition of RNF8 and RNF168 RING finger E3 ligases at DNA damage sites. Frontiers in genetics. 2013; 4:128. [PubMed: 23847653]

Blank JL, Liu XJ, Cosmopoulos K, Bouck DC, Garcia K, Bernard H, Tayber O, Hather G, Liu R, Narayanan U, et al. Novel DNA Damage Checkpoints Mediating Cell Death Induced by the NEDD8-Activating Enzyme Inhibitor MLN4924. Cancer Res. 2013; 73:225–234. [PubMed: 23100467]

Brown JS, Lukashchuk N, Sczaniecka-Clift M, Britton S, le Sage C, Calsou P, Beli P, Galanty Y, Jackson SP. Neddylation Promotes Ubiquitylation and Release of Ku from DNA-Damage Sites. Cell Rep. 2015; 11:704–714. [PubMed: 25921528]

Budman J, Chu G. Assays for nonhomologous end joining in extracts. Methods Enzymol. 2006; 408:430–444. [PubMed: 16793385]

Calhoun ES, Jones JB, Ashfaq R, Adsay V, Baker SJ, Valentine V, Hempen PM, Hilgers W, Yeo CJ, Hruban RH, et al. BRAF and FBXW7 (CDC4, FBW7, AGO, SEL10) mutations in distinct subsets of pancreatic cancer: potential therapeutic targets. Am J Pathol. 2003; 163:1255–1260. [PubMed: 14507635]

Chen ZJ, Sun LJ. Nonproteolytic functions of ubiquitin in cell signaling. Mol Cell. 2009; 33:275–286. [PubMed: 19217402]

Chiruvella KK, Liang Z, Wilson TE. Repair of double-strand breaks by end joining. Cold Spring Harbor perspectives in biology. 2013; 5:a012757. [PubMed: 23637284]

Critchlow SE, Bowater RP, Jackson SP. Mammalian DNA double-strand break repair protein XRCC4 interacts with DNA ligase IV. Curr Biol. 1997; 7:588–598. [PubMed: 9259561]

Cukras S, Morffy N, Ohn T, Kee Y. Inactivating UBE2M Impacts the DNA Damage Response and Genome Integrity Involving Multiple Cullin Ligases. PLoS One. 2014; 9:e101844. [PubMed: 25025768]

Davis AJ, Chen DJ. DNA double strand break repair via non-homologous end-joining. Transl Cancer Res. 2013; 2:130–143. [PubMed: 24000320]

Davis RJ, Welcker M, Clurman BE. Tumor suppression by the Fbw7 ubiquitin ligase: mechanisms and opportunities. Cancer Cell. 2014; 26:455–464. [PubMed: 25314076]

Deans AJ, Khanna KK, McNees CJ, Mercurio C, Heierhorst J, McArthur GA. Cyclin-dependent kinase 2 functions in normal DNA repair and is a therapeutic target in BRCA1-deficient cancers. Cancer Res. 2006; 66:8219–8226. [PubMed: 16912201]

Deshaies RJ, Joazeiro CA. RING domain E3 ubiquitin ligases. Annual review of biochemistry. 2009; 78:399–434.

Ferguson DO, Sekiguchi JM, Chang S, Frank KM, Gao Y, DePinho RA, Alt FW. The nonhomologous end-joining pathway of DNA repair is required for genomic stability and the suppression of translocations. Proc Natl Acad Sci U S A. 2000; 97:6630–6633. [PubMed: 10823907]

Foster RE, Nnakwe C, Woo L, Frank KM. Monoubiquitination of the nonhomologous end joining protein XRCC4. Biochem Biophys Res Commun. 2006; 341:175–183. [PubMed: 16412978]

Fukuchi M, Wanotayan R, Liu S, Imamichi S, Sharma MK, Matsumoto Y. Lysine 271 but not lysine 210 of XRCC4 is required for the nuclear localization of XRCC4 and DNA ligase IV. Biochem Biophys Res Commun. 2015

Garcia K, Blank JL, Bouck DC, Liu XJ, Sappal DS, Hather G, Cosmopoulos K, Thomas MP, Kuranda M, Pickard MD, et al. Nedd8-activating enzyme inhibitor MLN4924 provides synergy with mitomycin C through interactions with ATR, BRCA1/BRCA2, and chromatin dynamics pathways. Mol Cancer Ther. 2014; 13:1625–1635. [PubMed: 24672057]

Grim JE, Gustafson MP, Hirata RK, Hagar AC, Swanger J, Welcker M, Hwang HC, Ericsson J, Russell DW, Clurman BE. Isoform- and cell cycle-dependent substrate degradation by the Fbw7 ubiquitin ligase. J Cell Biol. 2008; 181:913–920. [PubMed: 18559665]

Hofmann RM, Pickart CM. Noncanonical MMS2-encoded ubiquitin-conjugating enzyme functions in assembly of novel polyubiquitin chains for DNA repair. Cell. 1999; 96:645–653. [PubMed: 10089880]

Jackson SP, Bartek J. The DNA-damage response in human biology and disease. Nature. 2009; 461:1071–1078. [PubMed: 19847258]

Jeggo PA, Geuting V, Lobrich M. The role of homologous recombination in radiation-induced double-strand break repair. Radiother Oncol. 2011; 101:7–12. [PubMed: 21737170]

Jia L, Sun Y. SCF E3 ubiquitin ligases as anticancer targets. Curr Cancer Drug Targets. 2011; 11:347–356. [PubMed: 21247385]

Jin J, Cardozo T, Lovering RC, Elledge SJ, Pagano M, Harper JW. Systematic analysis and nomenclature of mammalian F-box proteins. Genes Dev. 2004; 18:2573–2580. [PubMed: 15520277]

Jones S, Zhang X, Parsons DW, Lin JC, Leary RJ, Angenendt P, Mankoo P, Carter H, Kamiyama H, Jimeno A, et al. Core signaling pathways in human pancreatic cancers revealed by global genomic analyses. Science. 2008; 321:1801–1806. [PubMed: 18772397]

Junop MS, Modesti M, Guarne A, Ghirlando R, Gellert M, Yang W. Crystal structure of the Xrcc4 DNA repair protein and implications for end joining. EMBO J. 2000; 19:5962–5970. [PubMed: 11080143]

Kakarougkas A, Jeggo PA. DNA DSB repair pathway choice: an orchestrated handover mechanism. Br J Radiol. 2014; 87:20130685. [PubMed: 24363387]

Karnak D, Engelke CG, Parsels LA, Kausar T, Wei D, Robertson JR, Marsh KB, Davis MA, Zhao L, Maybaum J, et al. Combined Inhibition of Wee1 and PARP1/2 for Radiosensitization in Pancreatic Cancer. Clin Cancer Res. 2014; 20:5085–5096. [PubMed: 25117293]

Kirchgessner CU, Patil CK, Evans JW, Cuomo CA, Fried LM, Carter T, Oettinger MA, Brown JM. DNA-dependent kinase (p350) as a candidate gene for the murine SCID defect. Science. 1995; 267:1178–1183. [PubMed: 7855601]

Lieber MR. The mechanism of double-strand DNA break repair by the nonhomologous DNA end-joining pathway. Annual review of biochemistry. 2010; 79:181–211.

Liu P, Gan W, Guo C, Xie A, Gao D, Guo J, Zhang J, Willis N, Su A, Asara JM, et al. Akt-Mediated Phosphorylation of XLF Impairs Non-Homologous End-Joining DNA Repair. Mol Cell. 2015

Lobrich M, Shibata A, Beucher A, Fisher A, Ensminger M, Goodarzi AA, Barton O, Jeggo PA. gammaH2AX foci analysis for monitoring DNA double-strand break repair: strengths, limitations and optimization. Cell Cycle. 2010; 9:662–669. [PubMed: 20139725]

Mao JH, Perez-Losada J, Wu D, Delrosario R, Tsunematsu R, Nakayama KI, Brown K, Bryson S, Balmain A. Fbxw7/Cdc4 is a p53-dependent, haploinsufficient tumour suppressor gene. Nature. 2004; 432:775–779. [PubMed: 15592418]

Mao Z, Jiang Y, Liu X, Seluanov A, Gorbunova V. DNA repair by homologous recombination, but not by nonhomologous end joining, is elevated in breast cancer cells. Neoplasia. 2009; 11:683–691. [PubMed: 19568413]

Mari PO, Florea BI, Persengiev SP, Verkaik NS, Bruggenwirth HT, Modesti M, Giglia-Mari G, Bezstarosti K, Demmers JA, Luider TM, et al. Dynamic assembly of end-joining complexes requires interaction between Ku70/80 and XRCC4. Proc Natl Acad Sci U S A. 2006; 103:18597–18602. [PubMed: 17124166]

Nakayama KI, Nakayama K. Ubiquitin ligases: cell-cycle control and cancer. Nat Rev Cancer. 2006; 6:369–381. [PubMed: 16633365]

Nawrocki ST, Griffin P, Kelly KR, Carew JS. MLN4924: a novel first-in-class inhibitor of NEDD8-activating enzyme for cancer therapy. Expert Opin Investig Drugs. 2012; 21:1563–1573.

Ochi T, Blackford AN, Coates J, Jhujh S, Mehmood S, Tamura N, Travers J, Wu Q, Draviam VM, Robinson CV, et al. DNA repair. PAXX, a paralog of XRCC4 and XLF, interacts with Ku to promote DNA double-strand break repair. Science. 2015; 347:185–188. [PubMed: 25574025]

Ochi T, Wu Q, Blundell TL. The spatial organization of non-homologous end joining: from bridging to end joining. DNA Repair (Amst). 2014; 17:98–109. [PubMed: 24636752]

Perez-Losada J, Mao JH, Balmain A. Control of genomic instability and epithelial tumor development by the p53-Fbxw7/Cdc4 pathway. Cancer Res. 2005; 65:6488–6492. [PubMed: 16061623]

Pfeiffer P, Odersky A, Goedecke W, Kuhfittig-Kulle S. Analysis of double-strand break repair by nonhomologous DNA end joining in cell-free extracts from mammalian cells. Methods Mol Biol. 2014; 1105:565–585. [PubMed: 24623253]

Pierce AJ, Johnson RD, Thompson LH, Jasin M. XRCC3 promotes homology-directed repair of DNA damage in mammalian cells. Genes Dev. 1999; 13:2633–2638. [PubMed: 10541549]

Radhakrishnan SK, Jette N, Lees-Miller SP. Non-homologous end joining: emerging themes and unanswered questions. DNA repair. 2014; 17:2–8. [PubMed: 24582502]

Rajagopalan H, Jallepalli PV, Rago C, Velculescu VE, Kinzler KW, Vogelstein B, Lengauer C. Inactivation of hCDC4 can cause chromosomal instability. Nature. 2004; 428:77–81. [PubMed: 14999283]

Rooney S, Alt FW, Lombard D, Whitlow S, Eckersdorff M, Fleming J, Fugmann S, Ferguson DO, Schatz DG, Sekiguchi J. Defective DNA repair and increased genomic instability in Artemis-deficient murine cells. J Exp Med. 2003; 197:553–565. [PubMed: 12615897]

Sharma S, Raghavan SC. Nonhomologous DNA end joining in cell-free extracts. Journal of nucleic acids. 2010

Shinohara ET, Geng L, Tan J, Chen H, Shir Y, Edwards E, Halbrook J, Kesicki EA, Kashishian A, Hallahan DE. DNA-dependent protein kinase is a molecular target for the development of noncytotoxic radiation-sensitizing drugs. Cancer Res. 2005; 65:4987–4992. [PubMed: 15958537]

Soucy TA, Smith PG, Milhollen MA, Berger AJ, Gavin JM, Adhikari S, Brownell JE, Burke KE, Cardin DP, Critchley S, et al. An inhibitor of NEDD8-activating enzyme as a new approach to treat cancer. Nature. 2009; 458:732–736. [PubMed: 19360080]

Theys J, Yahyanejad S, Habets R, Span P, Dubois L, Paesmans K, Kattenbeld B, Cleutjens J, Groot AJ, Schuurbiers OC, et al. High NOTCH activity induces radiation resistance in non small cell lung cancer. Radiother Oncol. 2013; 108:440–445. [PubMed: 23891097]

Ulrich HD, Walden H. Ubiquitin signalling in DNA replication and repair. Nat Rev Mol Cell Biol. 2010; 11:479–489. [PubMed: 20551964]

VanDemark AP, Hofmann RM, Tsui C, Pickart CM, Wolberger C. Molecular insights into polyubiquitin chain assembly: crystal structure of the Mms2/Ubc13 heterodimer. Cell. 2001; 105:711–720. [PubMed: 11440714]

Wang J, Wakeman TP, Lathia JD, Hjelmeland AB, Wang XF, White RR, Rich JN, Sullenger BA. Notch promotes radioresistance of glioma stem cells. Stem Cells. 2010; 28:17–28. [PubMed: 19921751]

Wang WJ, Wu SP, Liu JB, Shi YS, Huang X, Zhang QB, Yao KT. MYC regulation of CHK1 and CHK2 promotes radioresistance in a stem cell-like population of nasopharyngeal carcinoma cells. Cancer Res. 2013; 73:1219–1231. [PubMed: 23269272]

Wang Z, Liu P, Inuzuka H, Wei W. Roles of F-box proteins in cancer. Nat Rev Cancer. 2014; 14:233–247. [PubMed: 24658274]

Wei D, Li H, Yu J, Sebolt JT, Zhao L, Lawrence TS, Smith PG, Morgan MA, Sun Y. Radiosensitization of human pancreatic cancer cells by MLN4924, an investigational NEDD8-activating enzyme inhibitor. Cancer Res. 2012; 72:282–293. [PubMed: 22072567]

Wei D, Zhang Q, Schreiber JS, Parsels LA, Abulwerdi FA, Kausar T, Lawrence TS, Sun Y, Nikolovska-Coleska Z, Morgan MA. Targeting mcl-1 for radiosensitization of pancreatic cancers. Transl Oncol. 2015; 8:47–54. [PubMed: 25749177]

Welcker M, Clurman BE. FBW7 ubiquitin ligase: a tumour suppressor at the crossroads of cell division, growth and differentiation. Nat Rev Cancer. 2008; 8:83–93. [PubMed: 18094723]

Williams GJ, Hammel M, Radhakrishnan SK, Ramsden D, Lees-Miller SP, Tainer JA. Structural insights into NHEJ: building up an integrated picture of the dynamic DSB repair super complex, one component and interaction at a time. DNA repair. 2014; 17:110–120. [PubMed: 24656613]

Woodbine L, Gennery AR, Jeggo PA. The clinical impact of deficiency in DNA non-homologous end-joining. DNA Repair (Amst). 2014; 16:84–96. [PubMed: 24629483]

Wu J, Zhang X, Zhang L, Wu CY, Rezaeian AH, Chan CH, Li JM, Wang J, Gao Y, Han F, et al. Skp2 E3 ligase integrates ATM activation and homologous recombination repair by ubiquitinating NBS1. Mol Cell. 2012; 46:351–361. [PubMed: 22464731]

Yu Y, Wang W, Ding Q, Ye R, Chen D, Merkle D, Schriemer D, Meek K, Lees-Miller SP. DNA-PK phosphorylation sites in XRCC4 are not required for survival after radiation or for V(D)J recombination. DNA Repair (Amst). 2003; 2:1239–1252. [PubMed: 14599745]

Zha S, Alt FW, Cheng HL, Brush JW, Li G. Defective DNA repair and increased genomic instability in Cernunnos-XLF-deficient murine ES cells. Proc Natl Acad Sci U S A. 2007; 104:4518–4523. [PubMed: 17360556]

Zhao Y, Morgan MA, Sun Y. Targeting Neddylation Pathways to Inactivate Cullin-RING Ligases for Anticancer Therapy. Antioxidants & redox signaling. 2014

Zhao Y, Sun Y. Cullin-RING Ligases as Attractive Anti-cancer Targets. Curr Pharm Des. 2013; 19:3215–3225. [PubMed: 23151137]

Zhao Y, Thomas HD, Batey MA, Cowell IG, Richardson CJ, Griffin RJ, Calvert AH, Newell DR, Smith GC, Curtin NJ. Preclinical evaluation of a potent novel DNA-dependent protein kinase inhibitor NU7441. Cancer Res. 2006; 66:5354–5362. [PubMed: 16707462]

Zhao Y, Xiong X, Sun Y. DEPTOR, an mTOR inhibitor, is a physiological substrate of SCF(betaTrCP) E3 ubiquitin ligase and regulates survival and autophagy. Mol Cell. 2011; 44:304–316. [PubMed: 22017876]

Zhou W, Wei W, Sun Y. Genetically engineered mouse models for functional studies of SKP1-CUL1-F-box-protein (SCF) E3 ubiquitin ligases. Cell research. 2013; 23:599–619. [PubMed: 23528706]

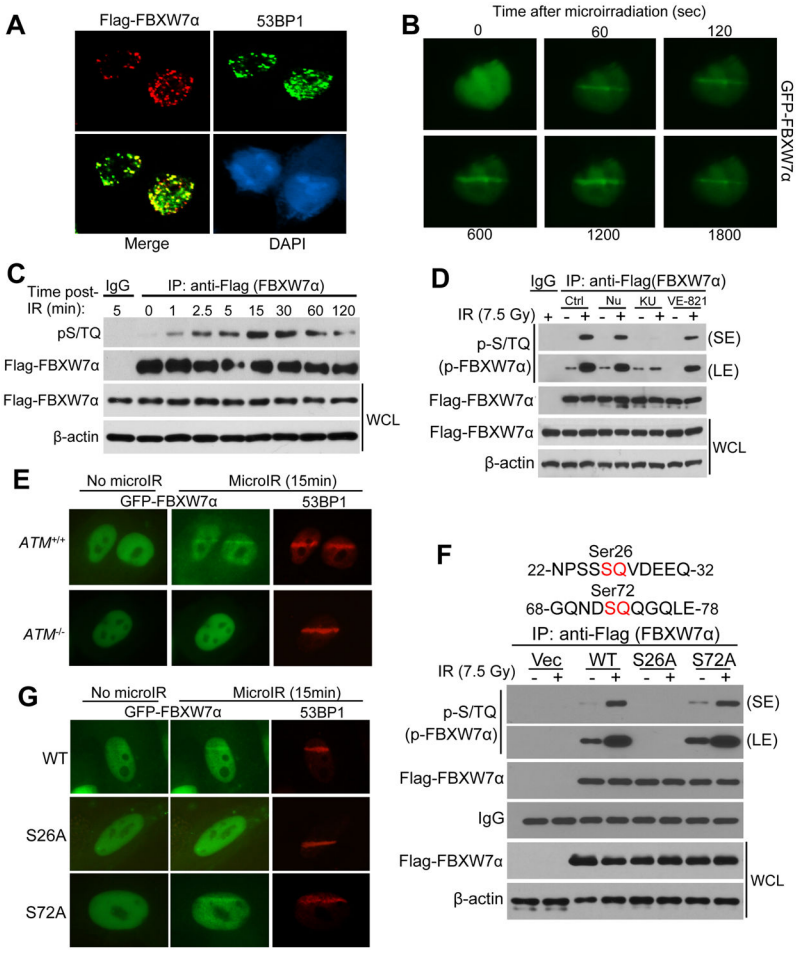

Figure 1. ATM-dependent recruitment of FBXW7α to DNA damage sites

(**A**) MiaPaCa-2 cells transfected with Flag-FBXW7α were exposed to IR (7.5 Gy) and fixed for immunofluorescence 15 minutes post-IR. Cells were co-stained for Flag-FBXW7 (red) and 53BP1 (green). (**B**) Accumulation of GFP-FBXW7α fusion protein along DNA damage 'tracks' after UVA laser microirradiation (microIR). (**C**) Flag-FBXW7α transfected MiaPaCa-2 cells were irradiated (7.5 Gy) and collected for immunoprecipitation (IP) and immunoblot (IB) with Flag and pS/TQ antibodies, respectively. (**D**) Cells were treated with DMSO, Nu7441 (1 μM, DNA-PKcs inhibitor), KU55933 (10 μM, ATM inhibitor) or VE-821 (10 μM, ATR inhibitor) for 1 hour pre- and 15 minutes post-IR and then collected for IP/IB as indicated. (**E**) GFP-FBXW7α accumulation at DNA damage sites after laser microIR was measured in AT fibroblasts. (**F**) MiaPaCa-2 cells were transiently transfected with Flag-FBXW7α-WT, S26A or S72A, followed by IP/IB after IR. (**G**) Localization of GFP-FBXW7α WT and mutants at DNA damage sites 15 minutes after microIR. Scale bars are 10 μm. (See also Figure S1.)

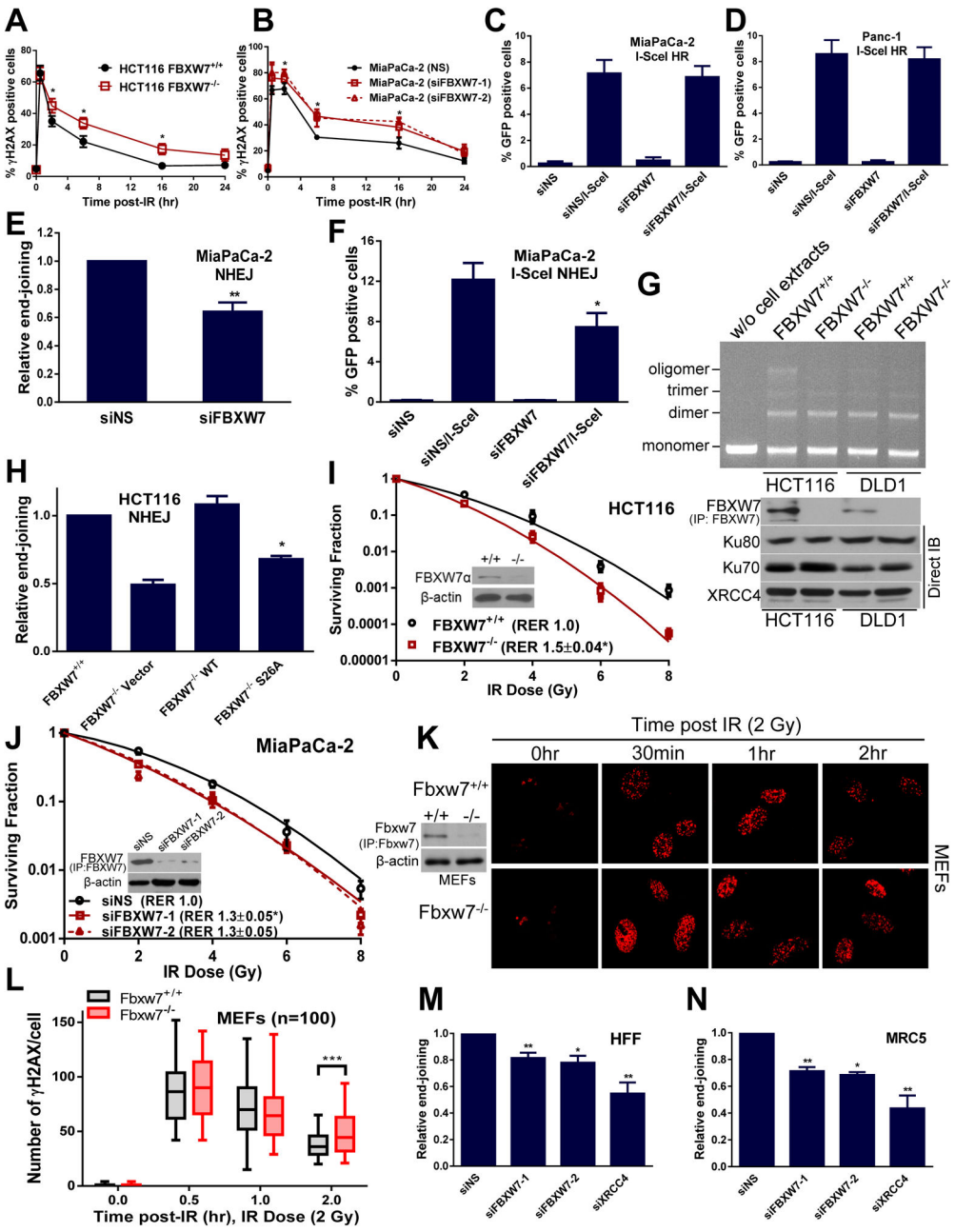

Figure 2. Depletion of FBXW7 leads to persistent γH2AX, impaired NHEJ, and radiosensitization

(**A, B**) FBXW7 isogenic HCT116 (A) or MiaPaCa-2 cells transfected with either non-specific (siNS) or FBXW7 siRNA (siFBXW7; two independent siRNAs) (B) were analyzed at the indicated times post-IR (6 Gy) for γH2AX positivity by flow cytometry. (**C–D**) MiaPaCa-2 and Panc-1 cells stably expressing the DR-GFP HR reporter were transfected with the indicated siRNAs and infected with adenovirus expressing I-SceI. The percentage of GFP-positive cells, indicating HR repair, was analyzed by flow cytometry (n = 2 independent experiments). (**E**) MiaPaCa-2 cells were transfected with siNS or siFBXW7. Forty-eight hours post-transfection, cells were further transfected with linearized-pEYFP

plasmid for 12 hours, followed by harvesting for qPCR to detect the ligated EYFP region, normalized to an uncut flanking DNA sequence. (**F**) Cells stably expressing the I-SceI NHEJ reporter were transfected with siNS or siFBXW7, infected with I-SceI expressing adenovirus, and analyzed for GFP positivity by flow cytometry. (**G**) Cell extracts were incubated with linearized (by EcoRI for a 2 hour digestion producing 5′ overhangs) pBlueScript vector. End-joining products appear as higher molecular weight bands. (**H**) NHEJ activity was assessed in FBXW7 isogenic HCT116 cells stably expressing FBXW7α WT or S26A mutant as described in panel E. (**I, J**) FBXW7 isogenic HCT116 (I) or MiaPaCa-2 cells transfected with siRNA (J) were treated with IR and processed for clonogenic survival 24 hours post-IR. The radiation enhancement ratio (RER) and surviving fraction are the mean ± SD/SE of 2–3 independent experiments. (**K–L**) MEF cells (wild type and FBXW7 null) were serum starved (24 hours) and then assessed for λH2AX foci by immunofluorescence at the indicated times post-IR (2 Gy). Scale bar, 5 μm. Similar results were observed with 6 Gy radiation (data not shown). (**M–N**) NHEJ activity was assessed in serum starved (24 hours) normal fibroblasts HFF (M) and MRC5 (N) with FBXW7 or XRCC4 depletion. (A–B, E–F, H–J, M–N) Data are the mean ± SE of 3 independent experiments. *p<0.05, **p<0.01, ***p<*0.001*. (See also Figure S2.)

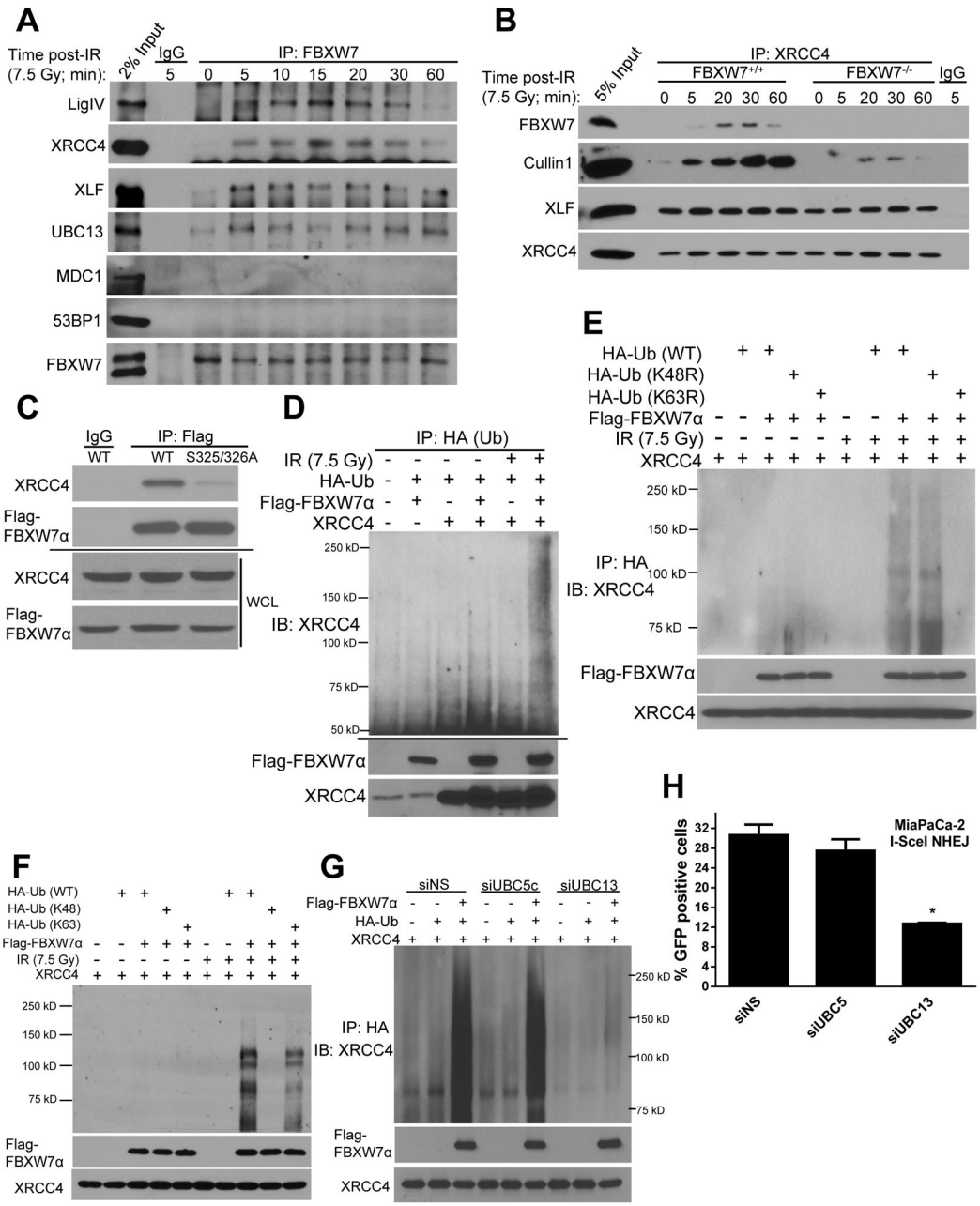

Figure 3. SCF^{FBXW7α} promotes XRCC4 polyubiquitylation via K63-linkage

(**A**) FBXW7α interacts with XRCC4, LigIV, XLF, and UBC13, but not MDC1 and 53BP1 endogenously in MiaPaCa-2 cells. IgG was used as the IP control. (**B**) MiaPaCa-2 cells were harvested for immunoprecipitation with XRCC4 antibody at the indicated times post-IR, followed by immunoblotting for the indicated proteins. (**C**) XRCC4 mutation in the FBXW7 binding motif (S325/326A) reduces FBXW7α-XRCC4 association. MiaPaCa-2 cells co-transfected with Flag-FBXW7α and XRCC4 WT or S325/326A mutant were irradiated and then collected for IP/IB. (**D**) FBXW7α promotes XRCC4 polyubiquitylation in response to radiation. MiaPaCa-2 cells transfected with various constructs were harvested 15 minutes

post-IR (7.5 Gy) for IP with HA antibody, followed by IB with XRCC4 antibody. (**E**) XRCC4 polyubiquitylation is via K63-ubiquitin linkage. Wild type or mutant (K48R, K63R) HA-tagged ubiquitin (HA-Ub) were used to define the type of ubiquitin linkage. (**F**) K63-only, but not K48-only ubiquitin mutant mediates XRCC4 polyubiquitylation upon IR treatment in MiaPaCa-2 cells. (**G**) MiaPaCa-2 cells transfected with non-specific, UBC5 or UBC13 siRNA were further transfected with the indicated constructs and harvested 15 minutes post-IR for *in vivo* ubiquitylation assays. (**H**) MiaPaCa-2 cells stably expressing an NHEJ reporter were transfected with non-specific, UBC5 or UBC13 siRNA and NHEJ repair efficiency was measured as described in Figure 2F (n = 2 independent experiments). (See also Figure S3.)

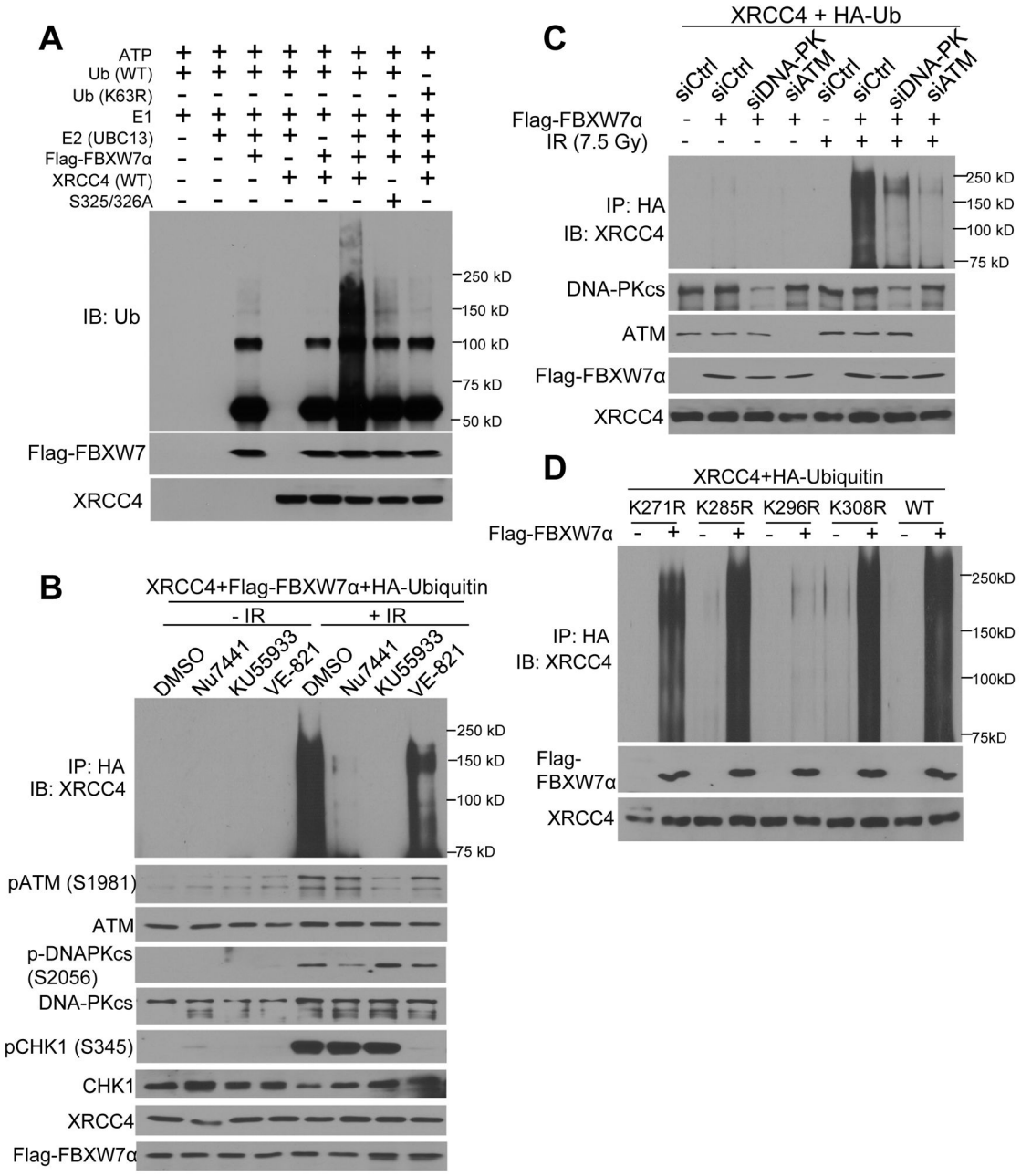

Figure 4. SCF^{FBXW7α} ubiquitylates XRCC4 at Lys296 in an ATM- and DNA-PKcs-dependent manner

(**A**) *In vitro* ubiquitylation assays were performed by incubating purified XRCC4 with ATP, ubiquitin, E1, and E2 in the presence or absence of E2, immunoprecipitated Flag-FBXW7 or XRCC4 followed by IB. Ub (K63R) and XRCC4 S325/326A were used as negative controls. (**B**) Pharmacological inhibition of DNA-PKcs or ATM by Nu7441 or KU55933, respectively inhibits XRCC4 ubiquitylation. MiaPaCa-2 cells transfected with the indicated constructs were pre-treated with inhibitors (1 hour) and irradiated (7.5 Gy). XRCC4 ubiquitylation was examined by IP with HA antibody, followed by IB for the indicated proteins. (**C**) Depletion of DNA-PKcs or ATM impairs XRCC4 polyubiquitylation. XRCC4

polyubiquitylation was assessed in cells treated with non-specific, DNA-PKcs, or ATM siRNAs. (**D**) K296 on XRCC4 is the ubiquitylation site of FBXW7α. Ubiquitylation of four XRCC4 lysine mutants (K271R, K285R, K296R, and K308R) was measured as described in Figure 3D. (See also Figure S4.)

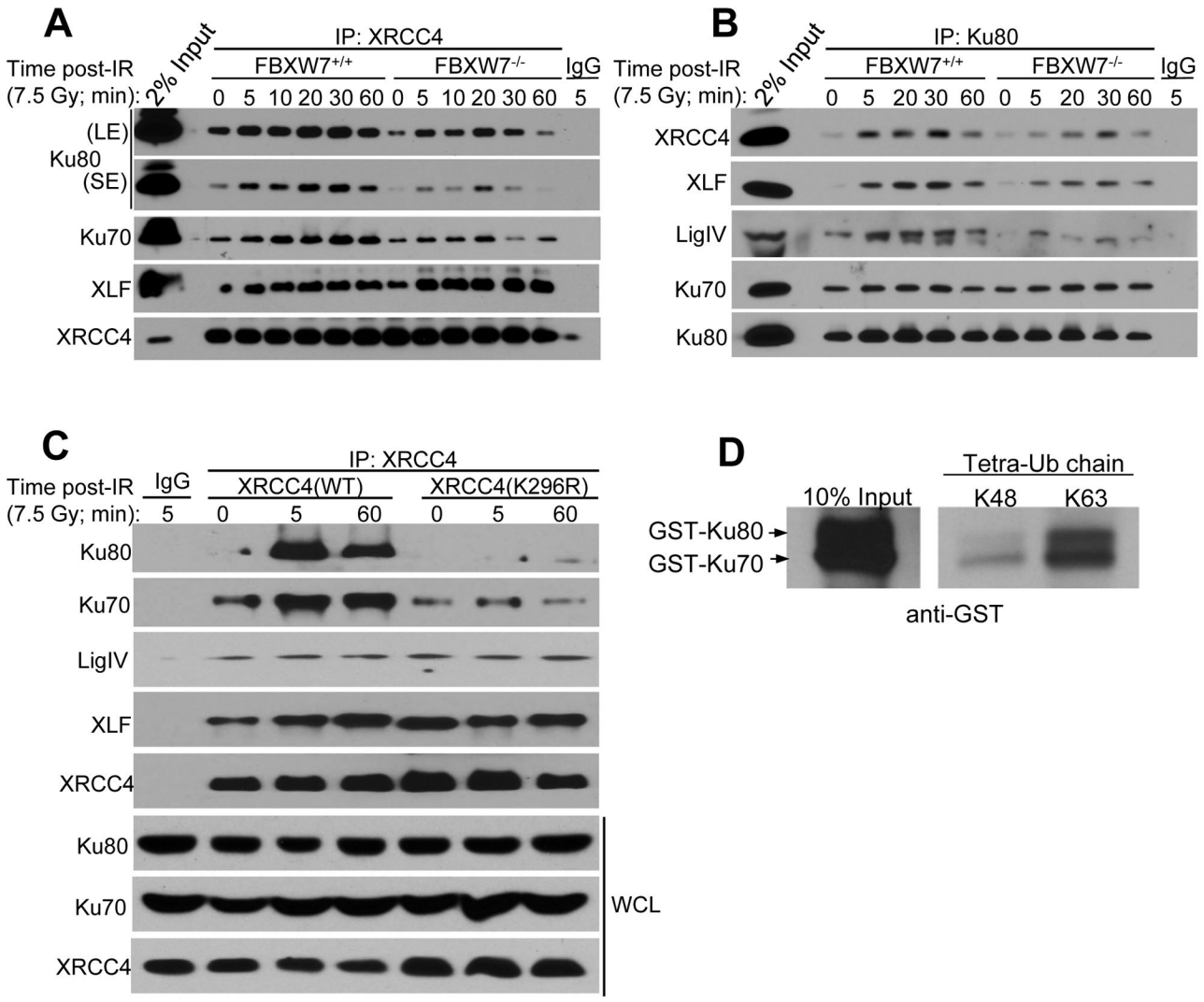

Figure 5. FBXW7α-mediated XRCC4 polyubiquitylation facilitates NHEJ complex formation

(**A–B**) FBXW7 isogenic HCT116 cells were irradiated (7.5 Gy) and collected for co-IP assays with XRCC4 or Ku80 antibody, followed by IB for NHEJ proteins. (**C**) K296 of XRCC4 is required for association with Ku70/80. XRCC4 WT and K296R mutants were expressed in MiaPaCa-2 cells and their interaction with endogenous NHEJ proteins after IR was examined by XRCC4 IP. (**D**) Purified GST-Ku70/K80 heterodimer proteins from Sf9 cells were incubated with agarose beads conjugated with tetra-ubiquitin K48 or K63, as indicated. Ku70/80 and tetra-ubiquitin chains were eluted by SDS sample buffer, followed by immunoblotting for GST. (See also Figure S5.)

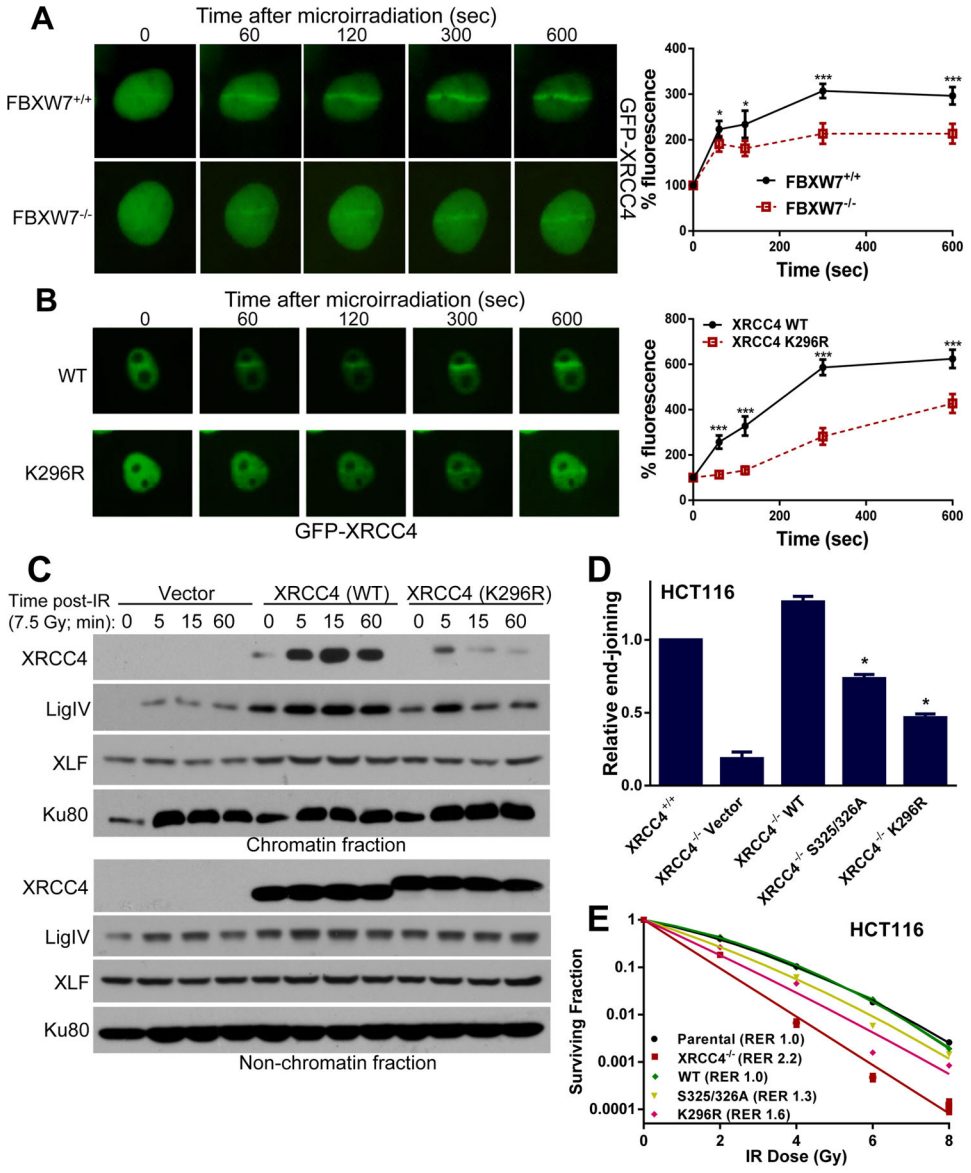

Figure 6. Ubiquitylation at K296 promotes XRCC4 chromatin association, NHEJ repair, and radiation survival

(**A**) GFP-XRCC4 localization along microIR DNA damage sites was monitored and quantified post-microIR in FBXW7 isogenic HCT116 cells. Data are plotted as the percentage increase in fluorescence (arbitrary units) at the site of microIR and are the mean ± SD of 5 cells. (**B**) K296R mutation impairs the recruitment of GFP-XRCC4 to DNA damage sites. GFP-XRCC4 WT or K296R were expressed in MiaPaCa-2 cells and their localization to microIR DNA damage sites was monitored post-microIR. (**C**) XRCC4 isogenic HCT116 cells, XRCC4 WT and K296R stable cells were treated with or without IR (6 Gy) and harvested at various time points for the isolation of non-chromatin and chromatin fraction, followed by immunoblot analysis. (**D**) NHEJ activity was assessed in XRCC4 isogenic HCT116 cells stably expressing XRCC4 WT or S325/326 or K296R mutants as described in Figure 2D (Data are the mean ± SE of 3 independent experiments) (**E**) XRCC4

isogenic HCT116 cells, as well as derived XRCC4 WT, S325/326A, and K296R stable cells were irradiated and 24 hours later processed for clonogenic survival. Data are presented as mean ± SD of 4 repeats. Scale bars are 10 μm. *p<0.05, ***p<0.001. (See also Figure S6.)

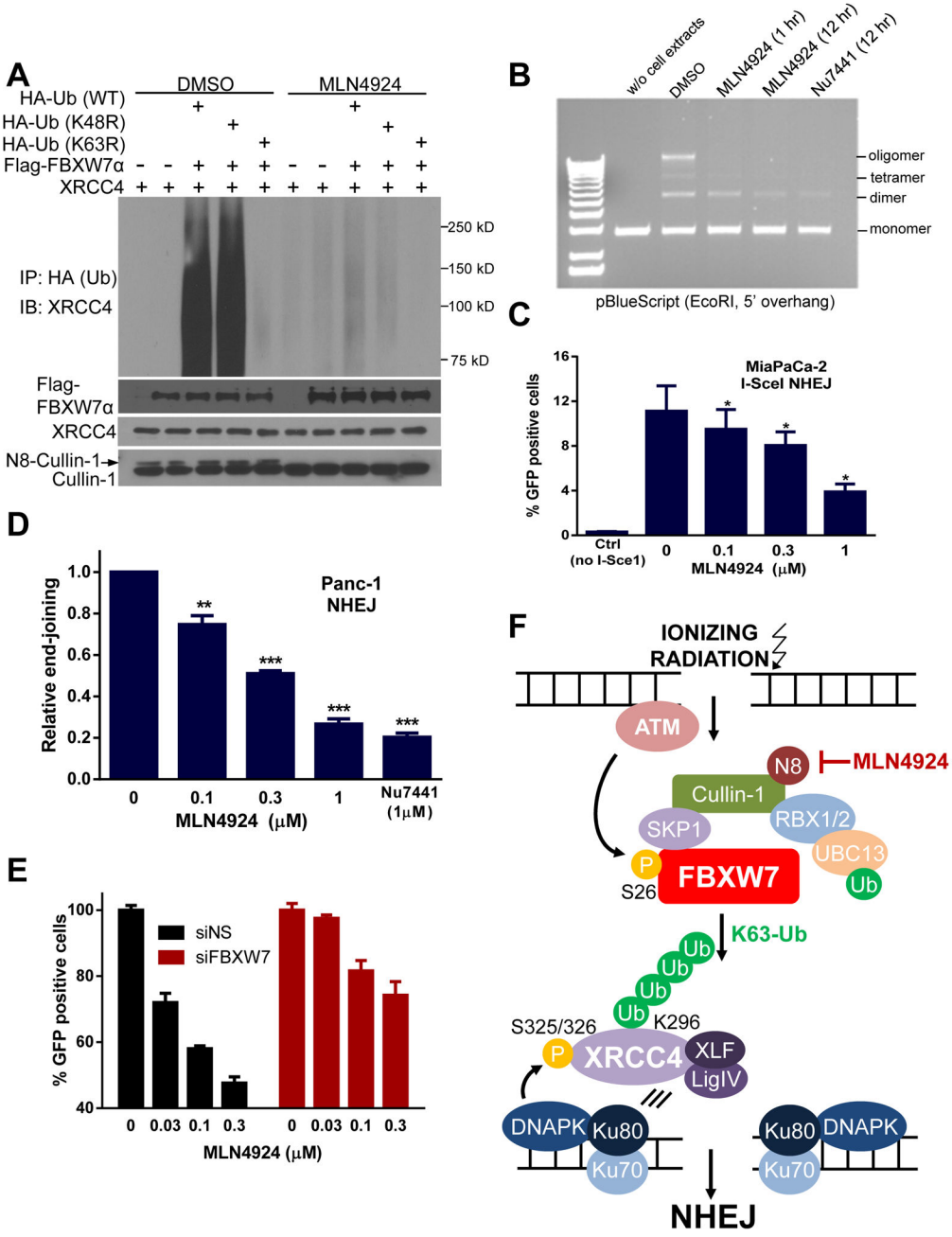

Figure 7. Pharmacological inhibition of SCF^{FBXW7} causes NHEJ inhibition

(**A**) MiaPaCa-2 cells transfected with WT, K48R or K63R HA-ubiquitin were pre-treated with MLN4924 (300 nM) for 6 hours, followed by IR (6 Gy) and collection for IP (15 minutes post-IR) with HA antibody, followed by IB. (**B**) MiaPaCa-2 cells were treated with drugs for the indicated times, followed by cell-free extract preparation. Linearized-pBlueScript vector (by EcoRI digestion) was incubated with the extracts for 2 hours. Reactions were subjected to agarose gel electrophoresis. (**C**) Cells stably expressing I-SceI NHEJ reporter were pre-treated for 1 hour with MLN4924, followed by infection with adenovirus expressing I-SceI and continued MLN4924 treatment for 24 hours. GFP positive

cells, indicative of NHEJ repair, were quantitated by flow cytometry. (**D**) Cells were pre-treated with drugs for 1 hour, then transfected with linearized-pEYFP plasmid (by NheI digestion), and analyzed by qPCR 12 hours later for the ligated pEYFP region normalized to an uncut flanking DNA sequence. (**E**) MiaPaCa-2 cells expressing the I-SceI NHEJ reporter were treated with non-specific (siNS) or FBXW7 siRNA and MLN4924. Data are the normalized mean percentage of MLN4924 inhibition for each RNAi condition. siFBXW7 alone caused 30% NHEJ inhibition relative to siNS. Data are the mean ± SD/SE of 2 (E) or 3 (C, D) independent experiments. *p<0.05, **p<0.01, ***p<0.001. (See also Figure S7.) (**F**) Proposed model for FBXW7 regulation of NHEJ. In response to radiation-induced DSBs, FBXW7α is phosphorylated (at S26) by ATM, leading to its recruitment to DSB sites. Locally enriched FBXW7 recognizes phosphorylated XRCC4 (by DNA-PKcs at S325/326) and together with other components of the SCF E3 ubiquitin ligase promotes K63-linked polyubiquitylation of XRCC4 at K296. Polyubiquitylated XRCC4 facilitates the association of XRCC4 (and LigIV/XLF) with the Ku70/80 heterodimer and DSBs to form an active NHEJ complex for effective repair. Pharmacologic (by MLN4924) or genetic (siRNA or genome deletion) inactivation of FBXW7α inhibits this pathway resulting in impaired NHEJ, persistent DSBs and increased radiation sensitivity. (See also Figure S7.)